EAST EUROPEAN JOURNAL OF PHYSICS
East Eur. J. Phys. **4**. 84-89 (2020) DOI:10.26565/2312-4334-2020-4-11

PACS: 62.65.+k; 63.50.+x; 62.30.+d

INFLUENCE OF DIELECTRIC SCREENINGS ON PHONON FREQUENCIES AND ACOUSTIC PROPERTIES OF Pd-BASED BULK METALLIC GLASSES

R.R. Koireng[a,b]*, P.C. Agarwal[c], Alpana Gokhroo[a]

[a]*Samrat Prithviraj Chauhan Government College, Ajmer-305001, Rajasthan, India*
[b]*National Institute of Education NCERT, New Delhi-110016, India*
[c]*Regional Institute of Education NCERT, Bhubaneswar-751022, Odisha, India*
**Corresponding Author: karenkrr@gmail.com*
Received September 10, 2020; accepted October 15, 2020

The phonon dispersion curves for bulk metallic glasses (BMGs) $Pd_{40}Ni_{10}Cu_{30}P_{20}$ and $Pd_{64}Ni_{16}P_{20}$ are computed for the longitudinal and transverse phonon frequencies using the simple model given by Bhatia and Singh. Different dielectric screening functions are employed for the longitudinal mode. We obtain the values of the force constants β and δ calculated from the elastic constants of the material of the respective BMGs for computing the dispersion curves. The computed phonon dispersion curves show appropriate behaviour for both the longitudinal and transverse modes. The transverse sound velocity and the longitudinal sound velocities with various dielectric screenings are calculated in the long wavelength region from the computed dispersion curves for both the BMGs. The first peak position of the static structure factor is predicted from the dispersion curves. The values of sound velocities and the first peak of the static structure factor estimated from the computed dispersion curves show excellent agreement with the experimental values reported in literature for the BMGs under consideration and the results may be used for correlating other properties of the BMGs.
KEYWORDS: Bulk metallic glass, dispersion curves, dielectric screening, elastic properties

The advent of bulk metallic glasses (BMGs) has attracted a lot of interest due to its novel properties and applications in diverse technological areas [1–3]. Pd-based BMGs due to their unique mechanical and thermal properties have shown potential applications as electrode, jewelry and medical materials [4-5]. However, the understanding of phonon dynamics and atomic structure configuration are essential for understanding their mechanical and thermal properties [6-9]. The phonon dynamics of metallic glasses have been studied experimentally [10-11] using neutron scattering. Theoretically computed phonon frequencies have been investigated by many researchers [12-17] for correlating them with mechanical and thermal properties in a variety of metallic glasses. Three main theoretical approaches, namely Hubbard and Beeby [15], Takeno and Goda [16] and that of Bhatia and Singh [8] are widely used for computing phonon frequencies of metallic glasses.

In this paper, the phonon dispersion curves of $Pd_{40}Ni_{10}Cu_{30}P_{20}$ and $Pd_{64}Ni_{16}P_{20}$ BMGs are computed using the simple model given by Bhatia and Singh [8]. This model assumes a central force which is effective between the nearest neighbours and a volume dependent force. Bhatia and Singh [8] determine the values of force constants δ and β using the value of longitudinal and transverse sound velocities along with the calculated value of force constant κ_e. However, in the approach adopted by us, we fix the values of force constants δ and β used in the computation of dispersion curves by using the value of bulk modulus (B) and shear modulus (G) of the respective BMGs along with the calculated value of κ_e. This method of determining the values of δ and β from the elastic modulii of the BMGS for computing phonon frequencies using the simple model is applied for the first time for the $Pd_{40}Ni_{10}Cu_{30}P_{20}$ and $Pd_{64}Ni_{16}P_{20}$ BMGs. The dielectric screening due to conduction electrons in the long wavelength region of the phonon frequencies is quite significant. To study its effect on the phonon frequencies, various dielectric screening functions [13] namely, Bhatia and Singh (BS), Hartree (H), Hubbard (HB), Geldart and Vosko (GV), self-consistent screening due to Shaw (SCS) and Overhauser (OH) are employed for the longitudinal mode.

The longitudinal sound velocities (V_L) are computed for different dielectric screenings and the transverse sound velocity (V_T) is computed from the longitudinal and transverse dispersion curves respectively in the long wavelength region for both the $Pd_{40}Ni_{10}Cu_{30}P_{20}$ and $Pd_{64}Ni_{16}P_{20}$ BMGs. The first peak position of the static structure factor $S(q)$ denoted by q_p provides key structural information and elastic properties of amorphous materials [7]. The value of q_p is estimated from the dispersion curves, where it occurs around the first minimum of the longitudinal vibration mode [9].

THEORY

The details of this theory of the simple model employed are given by Bhatia and Singh [8] and others [12-13]. The equations for the longitudinal phonon frequencies (ω_L) and transverse phonon frequencies (ω_T) as given by Bhatia and Singh [8] can be written as

$$\omega_{\mathrm{L}}^2 = \frac{2N}{\rho a^2}[\beta I_0 + \delta I_2] + \frac{\kappa_e K_{TF}^2 q^2 [G(qr_s)]^2}{\rho[q^2 + K_{TF}^2 \epsilon(q)]}, \quad (1)$$

and

$$\omega_{\mathrm{T}}^2 = \frac{2N}{\rho a^2}\left[\left(\beta + \frac{1}{2}\delta\right) I_0 - \frac{1}{2}\delta I_2\right], \tag{2}$$

here q is the momentum wave vector; β, δ and κ_e are force constants. β and δ are defined in terms of the first and second derivatives of inter-atomic potential $W(r)$ at $r = a$, as

$$\beta = \frac{\rho a^2}{2M}\left[\frac{1}{r}\frac{dW(r)}{dr}\right]_{r=a}, \tag{3}$$

$$\delta = \frac{\rho a^3}{2M}\left[\frac{d}{dr}\left(\frac{1}{r}\frac{dW(r)}{dr}\right)\right]_{r=a}. \tag{4}$$

In equation (1), the relevant force constant κ_e due to the conduction electrons based on the Thomas–Fermi model can be written as

$$\kappa_e = 4\pi n_e n_i z e^2 / K_{TF}^2, \tag{5}$$

where e is the electron charge, n_i is the ionic density, $n_e = n_i z$ is mean electron density and z is the mean valence of the glassy system; $K_{TF}^2 = (4\, k_F/\pi a_0)$ is the Thomas-Fermi screening length with a_0 as the Bohr radius.

The $[G(qr_s)]^2$ in equation (1) is the shape factor to take into account the cancellation effects of kinetic and potential energies inside the core of the ions and is of the form

$$[G(qr_s)]^2 = \left[\frac{3(\sin(qr_s) - (qr_s)\cos(qr_s))}{(qr_s)^3}\right]^2, \tag{6}$$

where $r_s = [3/(4\pi n_i)]^{1/3}$ is the radius of the Wigner- Seitz sphere.

The term $\epsilon(q)$ in equation (1) is the dielectric screening function. We employ various dielectric screenings [13] namely Bhatia and Singh (BS), Hartree (H), Hubbard (HB), Geldart and Vosko (GV), self-consistent screening due to Shaw (SCS) and Overhauser (OH) in equation (1) to study the effect on phonon frequencies in the long wavelength region.

In equations (1) and (2), I_n can be written as [8]

$$I_n = \int_0^{\pi} \sin\theta \cos^{\mathrm{n}}\theta \left[\sin^2\left(\frac{1}{2} qa\cos\theta\right)\right] \mathrm{d}\theta, \tag{7}$$

so that with $x = qa$, I_0 and I_2 are respectively,

$$I_0(x) = 1 - \frac{\sin x}{x},$$
$$I_2(x) = \frac{1}{3} - \sin x\left[\frac{1}{x} - \frac{2}{x^3}\right] - \frac{2\cos x}{x^2},$$

for the limiting case $q \to 0$, equations (1) and (2) give the longitudinal and transverse sound velocities respectively, $V_L(0) = \omega_L/q$ and $V_T(0) = \omega_T/q$ as

$$\rho V_L^2(0) = N\left(\frac{1}{3}\beta + \frac{1}{5}\delta\right) + \kappa_e, \tag{8}$$

$$\rho V_T^2(0) = N\left(\frac{1}{3}\beta + \frac{1}{15}\delta\right). \tag{9}$$

In terms of the elastic moduli of the glassy material [8]

$$C_{11} = \rho V_L^2(0) = B + \frac{4}{3}G, \tag{10}$$

$$C_{44} = \rho V_T^2(0) = G. \tag{11}$$

The value of β and δ can be determined using equations (8), (9), (10) and (11). The sound velocities for both $Pd_{40}Ni_{10}Cu_{30}P_{20}$ and $Pd_{64}Ni_{16}P_{20}$ BMGs are estimated for the longitudinal mode (V_L) with different dielectric screenings and transverse mode (V_T) in the long wavelength region from the respective dispersion curves. The first peak of the static structure factor for both the BMGs is also estimated from the dispersion curves.

CALCULATIONS

For the $Pd_{40}Ni_{10}Cu_{30}P_{20}$ BMG, the experimental values of B, G and ρ [2] are 172.60×10^9 Nm^{-2}, 35.50×10^9 Nm^{-2} and 9.259×10^3 kgm^{-3} respectively and for the $Pd_{64}Ni_{16}P_{20}$ BMG, the experimental values of B, G and ρ [2, 17] are taken as 172.00×10^9 Nm^{-2}, 32.80×10^9 Nm^{-2} and 10.08×10^3 kgm^{-3} respectively. The values of n_i is calculated using the

relation $\rho = n_i M$ and found to be 7.57×10^{28} m^{-3} for $Pd_{40}Ni_{10}Cu_{30}P_{20}$ and 7.26×10^{28} m^{-3} for $Pd_{64}Ni_{16}P_{20}$. The two BMGs under consideration are of FCC structure and using the relation $a^3 n_i = \sqrt{2}$, gives $a = 2.65\times10^{-10}$ m and $a = 2.69\times10^{-10}$ m for $Pd_{40}Ni_{10}Cu_{30}P_{20}$ and $Pd_{64}Ni_{16}P_{20}$ respectively.

The value of κ_e calculated using equation (5) for $Pd_{40}Ni_{10}Cu_{30}P_{20}$ with $z = 1.90$ is 153.50×10^9 Nm^{-2} and for $Pd_{64}Ni_{16}P_{20}$ with $z = 2.20$ is 182.75×10^9 Nm^{-2}. Taking N=12 for FCC structure for both the BMGs $Pd_{40}Ni_{10}Cu_{30}P_{20}$ and $Pd_{64}Ni_{16}P_{20}$, the values of the respective force constants β and δ for both the BMGs are obtained by substituting the respective values of B, G and κ_e in equations (8), (9), (10) and (11). Hence all the input parameters for computing phonon dispersion curves for both the BMGs are known and are listed in Table 1.

Table 1.

Parameters used for computing phonon dispersion curves of $Pd_{40}Ni_{10}Cu_{30}P_{20}$ and $Pd_{64}Ni_{16}P_{20}$ BMGs.

	$Pd_{40}Ni_{10}Cu_{30}P_{20}$	$Pd_{64}Ni_{16}P_{20}$
$n_i(10^{28}$ m$^{-3})$	7.57	7.26
κ_e (10^9 Nm^{-2})	153.50	182.75
k_F (10^{10} m^{-1})	1.62	1.68
r_s (10^{-10} m)	1.47	1.49
K_{TF}^2 (10^{20} m^{-2})	3.90	4.04
β (10^9 Nm^{-2})	5.01	8.18
δ (10^9 Nm^{-2})	19.33	0.11
z	1.90	2.20

RESULTS AND DISCUSSION

The phonon dispersion curves computed for the BMGs $Pd_{40}Ni_{10}Cu_{30}P_{20}$ and $Pd_{64}Ni_{16}P_{20}$ using the simple model given by Bhatia and Singh [8] are shown in Figure 1a and 1b respectively. The phonon frequency curves for the longitudinal mode employing different dielectric screening functions, namely Bhatia and Singh (BS), Hartree (H), Hubbard (HB), Geldart and Vosko (GV), self-consistent screening due to Shaw (SCS) and Overhauser (OH) for the BMGs $Pd_{40}Ni_{10}Cu_{30}P_{20}$ and $Pd_{64}Ni_{16}P_{20}$ are obtained on the basis of equation (1). Similarly, the phonon frequency curves for the transverse mode (T) for the $Pd_{40}Ni_{10}Cu_{30}P_{20}$ and $Pd_{64}Ni_{16}P_{20}$ BMGs are obtained on the basis of equation (2) without dielectric screening. The dispersion curves for both the longitudinal mode (ω_L-q) as well as the transverse mode (ω_T-q) show linear dispersion curves in the long wavelength region and reproduce all the characteristic features as shown in Figure 1a and 1b.

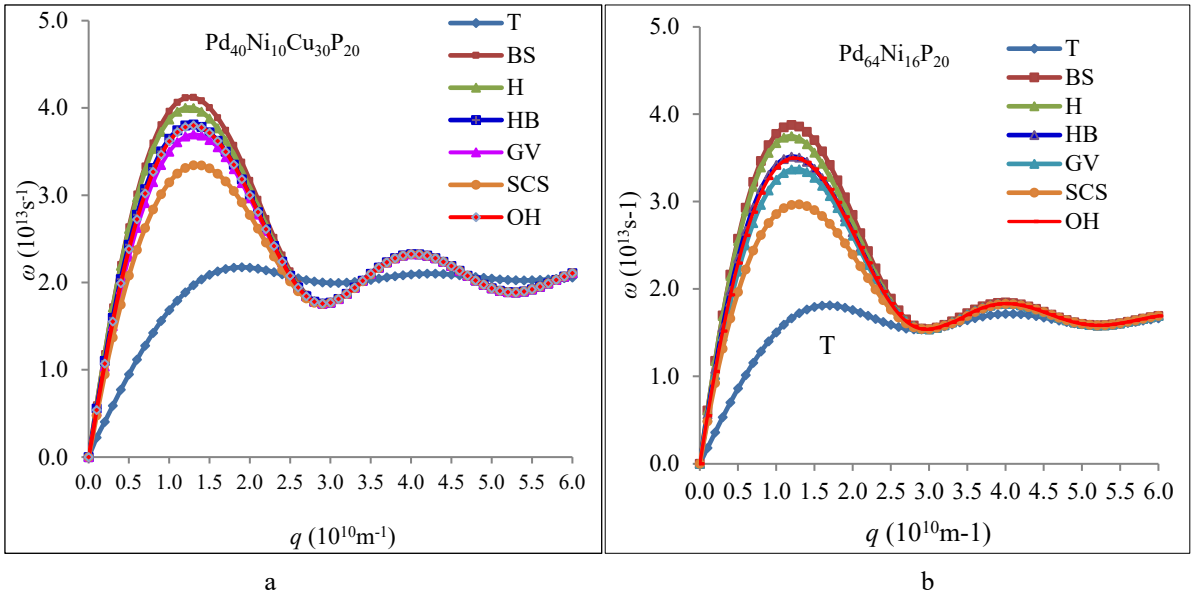

a b

Figure 1. The transverse (T) phonon frequencies on the basis of equation (2) and longitudinal phonon frequencies due to dielectric screenings viz. BS, H, HB, GV, SCS and OH on the basis of equation (1) for the BMGs (a)$Pd_{40}Ni_{10}Cu_{30}P_{20}$ and (b) $Pd_{64}Ni_{16}P_{20}$

As seen in Figure 1a and 1b, the dielectric screening functions have significant effect in the long wavelength region of the ω_L-q dispersion curves for both the $Pd_{40}Ni_{10}Cu_{30}P_{20}$ and $Pd_{64}Ni_{16}P_{20}$ BMGs. The height of the first peak of the longitudinal vibrations mode depends on the type of dielectric screenings employed for computing the phonon frequencies. From the Figure 1a and 1b, it is evident that the difference in ω_L-q curves for different dielectric screenings

for both the BMGs increases with the wave number q and becomes more prominent at the first maxima and starts decreasing, and the curves converge at the q value corresponding to the first minima of ω_L-q curves.

The position of the first peak of the ω_L-q curves for the $Pd_{40}Ni_{10}Cu_{30}P_{20}$ BMG are found at $q = 1.3\times10^{10}$ m^{-1} for BS, HB, GV, SCS and OH, and at $q = 1.2\times10^{10}$ m^{-1} for H. In the case of $Pd_{64}Ni_{16}P_{20}$ BMG, the position of the first peak for ω_L-q curves are found at $q = 1.2\times10^{10}$ m^{-1} for BS, H, HB and OH, and at $q = 1.3\times10^{10}$ m^{-1} for GV and SCS. The first minima of the ω_L-q curves for $Pd_{40}Ni_{10}Cu_{30}P_{20}$ and $Pd_{64}Ni_{16}P_{20}$ are obtained at $q = 2.9\times10^{10}$ m^{-1} and $q = 3.0\times10^{10}$ m^{-1} respectively, independent of the dielectric screenings employed.

The first peak position of ω_T-q curves for $Pd_{40}Ni_{10}Cu_{30}P_{20}$ and $Pd_{64}Ni_{16}P_{20}$ are obtained at $q = 1.9\times10^{10}$ m^{-1} and $q = 1.7\times10^{10}$ m^{-1} respectively. For both the BMGs $Pd_{40}Ni_{10}Cu_{30}P_{20}$ and $Pd_{64}Ni_{16}P_{20}$, the first peak position for ω_T-q curves is at a higher q value than the first peak position of ω_L-q curves for all dielectric screenings. As expected, the ω_T-q dispersion curves for both the BMGs increases and attain peak value with the increase in wave number q and thereafter gets saturated around the first peak with a small variation.

In the long wavelength region ($q\rightarrow0$) of the dispersion curves, the sound velocities of the longitudinal and transverse modes are estimated for both the BMGs. The values of longitudinal velocities (V_L) computed from the longitudinal dispersion curves for different dielectric screenings and the transverse velocity (V_T) computed from the transverse dispersion curves for both the BMGs $Pd_{40}Ni_{10}Cu_{30}P_{20}$ and $Pd_{64}Ni_{16}P_{20}$ are listed in Table 2. The dielectric screenings have significant effect on the longitudinal sound velocity. The experimental values of the longitudinal sound velocity for $Pd_{40}Ni_{10}Cu_{30}P_{20}$ is 4.874×10^5 cms^{-1} [2] and for $Pd_{64}Ni_{16}P_{20}$ is 4.560 cms^{-1} [2,17]. The values of V_L computed from the dispersion curves for both the BMGs under consideration show closeness to the experimental value for the dielectric screening due to OH. The value of V_L computed from the dispersion curves due to OH screening is 4.839×10^5 cms^{-1} for $Pd_{40}Ni_{10}Cu_{30}P_{20}$ and 4.606×10^5cms^{-1} for $Pd_{64}Ni_{16}P_{20}$. As shown in Table 2, the values of V_L computed for different dielectric screenings for both the BMGs are screening sensitive in the long wavelength region.

Table 2.

The transverse sound velocity (V_T) and longitudinal sound velocities (V_L) for different dielectric screenings for the BMGs $Pd_{40}Ni_{10}Cu_{30}P_{20}$ and $Pd_{64}Ni_{16}P_{20}$.

Dielectric screenings	$Pd_{40}Ni_{10}Cu_{30}P_{20}$		$Pd_{64}Ni_{16}P_{20}$	
	$V_L(10^5$ cms$^{-1})$	$V_T(10^5$ cms$^{-1})$	$V_L(10^5$ cms$^{-1})$	$V_T(10^5$ cms$^{-1})$
BS	5.358	1.827	5.181	1.735
H	5.313		5.133	
HB	4.949		4.722	
GV	4.664		4.405	
SCS	4.232		3.931	
OH	4.839		4.606	
Experimental	4.874[2]	1.959 [2]	4.560 [2,17]	1.790 [2,17]

The transverse sound velocity (V_T) computed from the slope of the dispersion curves in the elastic region for $Pd_{40}Ni_{10}Cu_{30}P_{20}$ is 1.827×10^5 cms^{-1} and for $Pd_{64}Ni_{16}P_{20}$ is 1.735×10^5cms^{-1}. The experimental values of transverse sound velocities reported for $Pd_{40}Ni_{10}Cu_{30}P_{20}$ and $Pd_{64}Ni_{16}P_{20}$ are 1.959 cms^{-1} [2] and 1.790 cms^{-1} [2,17] respectively. Thus, the computed transverse sound velocities are very close to the experimental values reported for $Pd_{40}Ni_{10}Cu_{30}P_{20}$ and $Pd_{64}Ni_{16}P_{20}$.

From the ω_L-q curves of the BMGs under consideration, we estimate the first peak position *(q_p)* of the static structure factor *S(q)*. The first minimum of ω_L-q curves occurs around the same value of the wave number q where the first peak *(q_p)* of the static structure factor *S(q)* occurs [9]. The position of the first minimum estimated from the ω_L-q curves for the BMGs $Pd_{40}Ni_{10}Cu_{30}P_{20}$ and $Pd_{64}Ni_{16}P_{20}$ occur at $q = 2.9\times10^{10}$ m^{-1} and $q = 3.0\times10^{10}$ m^{-1} respectively, independent of the dielectric screenings. The computed values of q_p for both the BMGs are given in Table 3. The experimental reported value of the first peak position q_p of the static structure factor for $Pd_{40}Ni_{10}Cu_{30}P_{20}$ is $q = 2.9\times10^{10}$ m^{-1} [7] (Table 3). However, no experimental data for the static structure factor of $Pd_{64}Ni_{16}P_{20}$ BMG is available, we estimate from the theoretical phonon dispersion curves to be at $q = 3.0\times10^{10}$ m^{-1}.

Table 3.

The position of the first peak (q_p) of static structure factor estimated from the dispersion curves of BMGs.

BMGs	q_p (10^{10} m^{-1})
$Pd_{40}Ni_{10}Cu_{30}P_{20}$	2.9, 2.9 [7]
$Pd_{64}Ni_{16}P_{20}$	3.0

The computed values of q_p for both the BMGs are slightly less than $2k_F$, where k_F is calculated using the relation, $k_F = (3\pi^2 n_e)^{1/3}$. The calculated values of k_F are 1.62 x10^{10} m^{-1} for $Pd_{40}Ni_{10}Cu_{30}P_{20}$ and 1.68 x10^{10} m^{-1} for $Pd_{64}Ni_{16}P_{20}$ (Table I). The ratio of $2k_F/q_p$ is 1.12 for both the BMGs $Pd_{40}Ni_{10}Cu_{30}P_{20}$ and $Pd_{64}Ni_{16}P_{20}$. This is in agreement with the

stability of metallic glasses [18]**.** Since the peak position of the structure factor provides key structural information in understanding atomic network for amorphous materials, it is used for correlating with elastic properties of BMGs [7]. From the results obtained from the dispersion curves, we can infer that the value of q_p is not affected by the dielectric screening functions, though the dielectric screenings have a significant effect on the values of the longitudinal sound velocities for the BMGs.

CONCLUSION

We have computed the phonon dispersion curves for $Pd_{40}Ni_{10}Cu_{30}P_{20}$ and $Pd_{64}Ni_{16}P_{20}$ BMGs employing various dielectric screenings using the simple model by Bhatia and Singh. The force constants δ and β used in the computation of the phonon frequencies are determined using the experimental values of bulk modulus (B) and shear modulus (G) along with the calculated value of force constant κ_e of the BMGs under consideration for the first time. The computed dispersion curves reproduce the main characteristic of phonon frequencies of transverse and longitudinal modes. The values of the transverse and longitudinal velocities estimated from the dispersion curves show excellent agreement with the experimental values reported for both the BMGs. The position of the first peak of the static structure factor for both the BMGs are estimated from the dispersion curves and show excellent agreement with the available value reported in literature for $Pd_{40}Ni_{10}Cu_{30}P_{20}$. Since the experimental data for phonon frequencies are rare and the limitation of the experimental techniques for describing the micro-structure of metallic glasses, the approach presented in this paper using the Bhatia and Singh model can be employed for computing phonon frequencies. It is expected that appropriate theoretical computation of phonon dispersion curves will give insight in understanding the structural information and elastic properties of metallic glasses.

ORCID IDs

R.R. Koireng, https://orcid.org/0000-0003-3112-1078; **P.C. Agarwal,** https://orcid.org/0000-0002-1166-2611;
Alpana Gokhroo, https://orcid.org/0000-0002-5871-0983

REFERENCES

[1] M. Telford, Materials Today, **7**, 36-43 (2004), https://doi.org/10.1016/S1369-7021(04)00124-5.
[2] W.H. Wang, Progress in Materials Science, **57**, 487-656 (2012), https://doi.org/10.1016/j.pmatsci.2011.07.001.
[3] M.M. Khan, A. Nemati, Z.U. Rahman, U.H. Shah, H. Asgar, and W. Haider, Critical Reviews in Solid State and Materials Science, **43**, 233-268 (2018), https://doi.org/10.1080/10408436.2017.1358149.
[4] A. Inoue, Z. M. Wang, and W. Zhang, Reviews on Advanced Materials Science, **18**, 1-9 (2008), http://www.ipme.ru/e-journals/RAMS/no_11808/inoue.pdf.
[5] L. Liu, A. Inoue, and T. Zhang, Materials, Transactions, **46**, 376-378 (2005), https://doi.org/10.2320/matertrans.46.376.
[6] Y.Q. Cheng, and E. Ma, Progress in Materials Science, **56**, 379- 473 (2011), https://doi.org/10.1016/j.pmatsci.2010.12.002.
[7] Y. Wu, H. Wang, Y. Cheng, X. Liu, X. Hui, T. Nieh, Y. Wang, and Z. Lu, Scientific Reports, **5**, 12137 (2015), https://doi.org/10.1038/srep12137.
[8] A.B. Bhatia, and R.N. Singh, Physical Review B, **31**, 4751- 4758 (1985), https://doi.org/10.1103/PhysRevB.31.4751.
[9] J. Hafner, Phyical Review B, **27**, 678- 695 (1983), https://doi.org/10.1103/PhysRevB.27.678.
[10] R. Babilas, D. Lukowiec, and L. Temleitner, Beilstein Journal of Nanotechnology, **8**, 1174-1182 (2017), https://doi.org/10.3762/bjnano.8.119.
[11] A. Gulenko, L.F. Chungong, J. Gao, I. Todd, A.C. Hannon, R.A. Martin, and J.K. Christie, Physical Chemistry Chemical Physics, **19**, 8504-8515 (2017), https://doi.org/10.1039/C6CP03261C.
[12] P.C. Agarwal, Physica B, **381**, 239-245 (2006), https://doi.org/10.1016/j.physb.2006.01.522.
[13] P.C. Agarwal, K.A. Aziz, and C.M. Kachhava, Acta Physica Hungarica, **72**, 183-192 (1992), https://doi.org/10.1007/BF03054162.
[14] A.M. Vora, and A.L. Gandhi, Armenian Journal of Physics, **12**, 289-294 (2019), http://ajp.asj-oa.am/1078/1/AMV_ALG_Armenian_Journal_of_Physics_pdf.pdf
[15] J. Hubbard, and J.L. Beeby, Journal of Physics C, **2**, 556-574 (1969), https://doi.org/10.1088/0022-3719/2/3/318.
[16] S. Takeno, and M. Goda, Progress of Theoretical Physics, **45**, 331-352 (1971), https://doi.org/10.1143/PTP.45.331.
[17] H.S. Chen, J.T. Krause, and E. Colemen, Journal of Non-Crystalline Solids, **18**, 157-171 (1975), https://doi.org/10.1016/0022-3093(75)90018-6.
[18] W.H. Wang, C. Dong, and C.H. Shek, Materials Science and Engineering: R: Reports **44**, 45-89 (2004), https://doi.org/10.1016/j.mser.2004.03.001.

ВПЛИВ ДІЕЛЕКТРИЧНОЇ ЕКРАНІЗАЦІЇ НА ФОНОННІ ЧАСТОТИ І АКУСТИЧНІ ВЛАСТИВОСТІ МЕТАЛІЧНИХ СТЕКОЛ НА ОСНОВІ Pd

Р.Р. Койренг[a,b], П.С. Агарвал[c], Альпана Гокру[a]

[a]Урядовий коледж Самрата Притвіраджа Чаухана, Аджмер-305001, Раджастан, Індія
[b]Національний інститут освіти (NCERT), Нью-Делі-110016, Індія
[c]Регіональний інститут освіти (NCERT), Бхубанешвар-751022, Одіша, Індія

Криві дисперсії фононів для об'ємних металевих стекол (ОМС) $Pd_{40}Ni_{10}Cu_{30}P_{20}$ та $Pd_{64}Ni_{16}P_{20}$ обчислюються для поздовжньої та поперечної частот фононів за допомогою простої моделі, наданої Бхатією та Сінгхом. Для поздовжнього режиму використовуються різні функції діелектричного екранування. Ми отримали значення силових констант β і δ, розрахованих з пружних констант матеріалу відповідних ОМС для обчислення кривих дисперсії. Обчислені криві дисперсії фононів демонструють належну поведінку як для поздовжньої, так і для поперечної мод. Поперечна швидкість звуку та

поздовжні швидкості звуку з різним діелектричним екрануванням обчислюються в області довжини довжини хвилі з обчислених кривих дисперсії для обох ОМС. Положення першого піка коефіцієнта статичної структури передбачено з дисперсійних кривих. Значення швидкостей звуку та перший пік коефіцієнта статичної структури, розраховані на основі обчислених дисперсійних кривих, показують чудову узгодженість з експериментальними значеннями, що наявні в літературі для розглянутих ОМС, і результати можуть бути використані для кореляції інших властивостей ОМС.
КЛЮЧОВІ СЛОВА: об'ємне металеве скло, дисперсійні криві, діелектричний екран, еластичні властивості

ВЛИЯНИЕ ДИЭЛЕКТРИЧЕСКОЙ ЭКРАНИРОВКИ НА ФОНОННЫЕ ЧАСТОТЫ И АКУСТИЧЕСКИЕ СВОЙСТВА МЕТАЛЛИЧЕСКИХ СТЕКОЛ НА ОСНОВЕ Pd

Р.Р. Койренг[a,b], П.С. Агарвал[c], Альпана Гокро Gokhroo[a]

[a]Урядовий колледж Самрат Притвираджа Чаухан, Аджмер-305001, Раджастан, Индия
[b]Национальний институт образования (NCERT), Нью-Дели-110016, Индия
[c]Региональний институт образования (NCERT), Бхубанешвар-751022, Одиши, Индия

Кривые дисперсии фононов для объемных металлических стекол (ОМС) $Pd_{40}Ni_{10}Cu_{30}P_{20}$ и $Pd_{64}Ni_{16}P_{20}$ исчисляются для продольной и поперечной частот фононов с помощью простой модели, предоставленной Бхатия и Сингхом. Для продольного режима используются различные функции диэлектрического экранирования. Мы получили значения силовых констант силы β и δ, рассчитанных по упругим константам материала соответствующих ОМС для вычисления кривых дисперсии. Вычисленные кривые дисперсии фононов демонстрируют надлежащее поведение как для продольной, так и для поперечной мод. Поперечная скорость звука и продольные скорости звука с разным диэлектрической экранированием исчисляются в области длины длины волны из вычисленных кривых дисперсии для обеих ОМС. Положение первого пика коэффициента статической структуры предсказано из дисперсионных кривых. Значения скоростей звука и первый пик коэффициента статической структуры, рассчитанные на основе вычисленных кривых дисперсии, показывают хорошее согласие с экспериментальными значениями, имеющиеся в литературе для рассматриваемых ОМС, и результаты могут быть использованы для корреляции других свойств ОМС.
КЛЮЧЕВЫЕ СЛОВА: объемное металлическое стекло, дисперсионные кривые, диэлектрический экран, эластичные свойства